



**HAL**  
open science

## Bioinjection treatment: Effects of post-injection residual stress on left ventricular wall stress

Lik Chuan Lee, Samuel T. Wall, Martin Genet, Andy Hinson, Julius M. Guccione

### ► To cite this version:

Lik Chuan Lee, Samuel T. Wall, Martin Genet, Andy Hinson, Julius M. Guccione. Bioinjection treatment: Effects of post-injection residual stress on left ventricular wall stress. *Journal of Biomechanics*, 2014, 47 (12), pp.4. 10.1016/j.jbiomech.2014.06.026 . hal-01196372

**HAL Id: hal-01196372**

**<https://hal.science/hal-01196372>**

Submitted on 5 Jan 2017

**HAL** is a multi-disciplinary open access archive for the deposit and dissemination of scientific research documents, whether they are published or not. The documents may come from teaching and research institutions in France or abroad, or from public or private research centers.

L'archive ouverte pluridisciplinaire **HAL**, est destinée au dépôt et à la diffusion de documents scientifiques de niveau recherche, publiés ou non, émanant des établissements d'enseignement et de recherche français ou étrangers, des laboratoires publics ou privés.

1 **BIOINJECTION TREATMENT: EFFECTS OF POST-INJECTION RESIDUAL STRESS**  
2 **ON LEFT VENTRICULAR WALL STRESS**

3 **Lik Chuan Lee<sup>1,2,3</sup>, Samuel T. Wall<sup>4</sup>, Martin Genet<sup>1,2,3,5</sup>, Andy Hinson<sup>6</sup> and Julius M.**  
4 **Guccione<sup>1,2,3</sup>**

5 Department of Surgery<sup>1</sup>, Bioengineering<sup>2</sup> and Medicine<sup>3</sup> University of California, San  
6 Francisco, CA; Simula Research Laboratory<sup>4</sup>, Oslo, Norway; Marie-Curie Outgoing  
7 fellow<sup>5</sup>; Lonestar Heart Inc<sup>6</sup>.

8

9

10

11 **Word count: 3729**

12

13

14

15

16

17

18

19

20

21

22

23

24 **Corresponding Author:**

25 Lik Chuan, Lee, PhD

26 Department of Surgery, School of Medicine,

27 University of California, San Francisco,

28 Mount Zion Harold Brunn Institute for Cardiovascular Research,

29 1657 Scott St., Room 219,

30 San Francisco, CA 94143,

31 Phone: +1 (510) 316-2102

32 Email: [LikChuan.Lee@ucsfmedctr.org](mailto:LikChuan.Lee@ucsfmedctr.org)

33

34 **ABSTRACT**

35

36 Injection of biomaterials into diseased myocardium has been associated with decreased myofiber  
37 stress, restored left ventricular (LV) geometry and improved LV function. However, its exact  
38 mechanism(s) of action remained unclear. In this work, we present the first patient-specific  
39 computational model of biomaterial injection that accounts for the possibility of residual strain  
40 and stress introduced by this treatment. We show that the presence of residual stress can create  
41 more heterogeneous regional myofiber stress and strain fields. Our simulation results show that  
42 the treatment generates low stress and stretch areas between injection sites, and high stress and  
43 stretch areas between the injections and both the endocardium and epicardium. Globally, these  
44 local changes are translated into an increase in average myofiber stress and its standard deviation  
45 (from  $6.9 \pm 4.6$  to  $11.2 \pm 48.8$  kPa and  $30 \pm 15$  to  $35.1 \pm 50.9$  kPa at end-diastole and end-  
46 systole, respectively). These results suggest that the residual stress and strain possibly generated  
47 by biomaterial injection treatment can have large effects on the regional myocardial stress and  
48 strain fields, which may be important in the remodeling process.

49

50

51

52 **Keywords:** Congestive heart failure, biomaterial injection, left ventricular wall stress,  
53 mathematical modeling, magnetic resonance imaging.

54

55 **1. INTRODUCTION**

56 Injection of materials into the myocardium as a treatment for heart diseases has generated  
57 considerable interest over recent years. The injection of biomaterials, which range from  
58 biological materials e.g., Alginate (Landa et al., 2008) and Fibrin (Christman et al., 2004), to  
59 synthetic hydrogels (Jiang et al., 2009), have shown positive outcomes in animal studies.  
60 Recently, significant reverse remodeling – 50% reduction in end-diastolic volume (EDV) and  
61 end-systolic volume (ESV) – in patients suffering from dilated cardiomyopathy was observed as  
62 early as 3 months after injection of Algiysl-LVR™ (a calcium-sodium alginate hydrogel) and  
63 Coronary Artery Bypass Grafting (Lee et al., 2013a).

64  
65 Despite these favorable outcomes, the exact mechanism(s) of action of the injection treatment  
66 remain(s) unclear. While the treatment’s primary rationale is to provide support to the diseased  
67 myocardium to reduce ventricular wall stress (widely believed to be responsible for adverse  
68 cardiac remodeling), there are also suggestions that these injected biomaterials can create a  
69 “healthier micro-environment through stress shielding” that increases capillary and arteriole  
70 densities (Nelson et al., 2011). Thus, the effects of this treatment need to be better understood,  
71 especially because of its potential as an effective treatment for heart diseases.

72  
73 Computational modeling has been used to better understand the effects of injecting material into  
74 the myocardium (Kortsmit et al., 2012; Wall et al., 2006; Wenk et al., 2009). These modeling  
75 studies generally support the primary rationale of the injection treatment: helping to provide  
76 support to the myocardium through thickening of the ventricular wall to reduce ventricular wall  
77 stress. However, these studies did not include the possible effects of residual stress that could  
78 occur when injections are introduced into the myocardium.

79  
80 Injectable biomaterials usually begin in a viscous liquid that solidifies through chemical changes  
81 *in situ* to form a solid hydrogel (Christman et al., 2004; Lee et al., 2013b). When injected, these  
82 liquids are forced into the myocardium, creating new space to accommodate the bleb of material.  
83 As such, residual stress can be introduced during this process, especially when the void that  
84 accommodates the injection has an initial volume smaller than the injected volume itself.  
85 Although the myocardial extracellular space (~ 24% of the tissue space) consists of about 6%

86 “empty” space devoid of any structural components (Frank and Langer, 1974) - about 2.7 ml for  
87 a left ventricular (LV) wall volume of 190 ml in the patient-specific model described here, they  
88 are interspersed within the myocardium and the local “empty” space is substantially smaller.  
89 Hence, it is likely that residual stress could be present when the injection volume  $\sim 0.3$  ml (Lee  
90 et al., 2013a) is greater than the local “empty” or void space.

91

92 The primary aims of this paper are twofold: first, to describe a methodology to model the effects  
93 of post-injection residual stress, and second, to highlight the possible effects of residual stress on  
94 local myofiber stress and stretch fields.

95

96

## 97 **2. METHODS AND RESULTS**

### 98 **2.1 Finite element model of the LV**

99 A patient-specific finite element (FE) model of the LV was constructed based on the baseline  
100 magnetic resonance (MR) images of patient 1 described in Lee et al. (2013a). The patient was  
101 diagnosed with NYHA class III heart failure and had ischemic cardiomyopathy, hypertension,  
102 hyperlipidemia and renal insufficiency. The LV was modeled using 110,976 trilinear hexahedral  
103 elements and the FE mesh was graded so that its mesh density was 4 times higher at the mid-LV  
104 (where the injections are located) (**Figure 1a**).

105 Nearly incompressible and transversely isotropic hyperelastic material laws for the passive  
106 (Guccione et al., 1991) and active myocardium (Guccione et al., 1993) were used to model the  
107 mechanical behavior of the LV during a cardiac cycle. The material passive stiffness ( $C$ ) and the  
108 tissue contractility ( $T_{\max}$ ) were chosen so that the predicted LV volumes (without injection)  
109 matched the corresponding EDV (197ml) and ESV (122ml) measured from MR images. All  
110 other parameters had values equal to those used in large animal studies (Sun et al., 2009) and  
111 human study (Wenk et al., 2012).

112 Local fiber direction was defined on the local tangent plane by prescribing a fiber angle taken  
113 with respect to the local circumferential vector running counterclockwise when viewed in the  
114 base-to-apex direction. In the entire LV, the fiber angle varied linearly from the endocardium

115 (60°) to the epicardium (-60°) (Streeter et al., 1969) (**Figure 1b**). The epicardial-base edge was  
116 fixed, whereas the base displacement was constrained in the out-of-plane direction.

117 Three simulation cases, namely, BASELINE, RESIDUAL and NO-RESIDUAL were performed.  
118 BASELINE was defined to be the case before injections. RESIDUAL and NO-RESIDUAL  
119 corresponded to the post-injection cases with and without the effects of residual stress,  
120 respectively.

121

## 122 **2.2 Modeling injections into the LV**

123 The LV wall was meshed with spherical voids at the mid LV (halfway between the base and the  
124 apex) and the voids were filled with hexahedral elements. The finite element meshes of the voids  
125 and the LV wall have matching nodes at their common interface. There were a total of 12 voids,  
126 each with an arbitrarily prescribed radius of 1mm (**Figure 1c**).

127 To model the effects arising from post-injection residual stress (RESIDUAL), the hexahedral  
128 elements in the void were first prescribed with a dummy material law and a spherical  
129 displacement field was then imposed to dilate each void to an arbitrary prescribed injection  
130 volume of 0.02 ml. Thereafter, stresses were initialized to zero in the elements defining the void  
131 and these elements were prescribed with a material law describing the hydrogel injections. In  
132 other words, the elements within the void now define the injected hydrogel. The hydrogel  
133 injections were modeled using nearly incompressible Mooney-Rivlin material law with  
134 previously obtained parameters (Wenk et al., 2009) from Alginate experiments. Then, the  
135 spherical displacement field was removed to allow the injections and the LV to deform until a  
136 force-equilibrium was reached (**Figure 1d**). This resultant configuration is defined to be the  
137 unloaded (but not stress-free) configuration. In NO-RESIDUAL, stresses of both the injections  
138 and LV wall were initialized to zero from the unloaded configuration of the RESIDUAL case.

139 End-diastole (ED) and end-systole (ES) were simulated in all 3 cases by imposing a pressure  
140 boundary condition of 20 mm Hg and 125 mm Hg at the endocardial wall in the unloaded  
141 configuration, respectively. All simulations were performed using LS-DYNA (Livermore

142 Software Technology Corporation, Livermore, CA) with the passive and active myocardial  
143 material law implemented as a user-defined material subroutine.

144

### 145 **2.3 Effect on Global Stretch and Stress in Myofiber and Cross-myofiber directions.**

146 Stretch and stress in both the myofiber and cross-myofiber directions were averaged over the  
147 entire LV at ED and ES for BASELINE, RESIDUAL and NO-RESIDUAL (**Table 1**). The  
148 average stress and stretch (at ES and ED) were not very different between BASELINE and NO-  
149 RESIDUAL in both the myofiber and cross-myofiber directions. However, the average ED  
150 myofiber stress of RESIDUAL ( $11.2 \pm 48.8$  kPa) was nearly twice as large as that of BASELINE  
151 ( $6.9 \pm 4.6$  kPa), whereas the average ES myofiber stress of RESIDUAL ( $35.1 \pm 50.9$  kPa) was  
152 17% higher than that of BASELINE ( $30 \pm 15$  kPa). Similar trend was also observed for the  
153 cross-myofiber stress of RESIDUAL, which was higher than BASELINE. The average ED and  
154 ES stretch of RESIDUAL was not very different from that of BASELINE in both the myofiber  
155 and cross-myofiber directions. In general, both ES and ED stress and stretch in RESIDUAL had  
156 larger values of standard deviation than BASELINE and NO-RESIDUAL.

157

### 158 **2.4 Effect on Local Myofiber Stretch and Stress**

159 The substantially larger standard deviation found in RESIDUAL suggests that the myofiber  
160 stress and stretch were more heterogeneous than the other 2 cases. Moreover, the significantly  
161 larger change in fiber stress than in fiber stretch indicates that out-of-fiber-direction tensions and  
162 shear-stress components must be activated.

163 Closer inspection of the myofiber stretch and stress fields reveals an organized pattern in the  
164 injection region, particularly in RESIDUAL when compared to NO-RESIDUAL (**Figures 2 and**  
165 **3**). In RESIDUAL, the myofiber stretch was substantially decreased and was less than unity at  
166 the mid wall between injections at both ED and ES. At ES, the myofiber stretch was elevated in  
167 the transmural direction between the injections and both the endocardium and epicardium. The  
168 ES myofiber stress field displayed similar pattern as that of the ES myofiber stretch.  
169 Contrastingly, ED myofiber stress did not decrease substantially between injections at the mid

170 wall and was elevated in the transmural direction between the injections and both epicardium and  
171 endocardium.

172 Without residual stress (NO-RESIDUAL), the myofiber stretch and stress fields at the injection  
173 region were largely similar to those in BASELINE, with the exception that the ED and ES  
174 myofiber stress between injections was slightly lower than in BASELINE (**Figure 3**).

175

## 176 **2.5 Effect of void-to-injection size ratio on myofiber stress**

177 The myofiber stress is also sensitive to the void-to-injection size ratio. By keeping the void size  
178 constant, both global ES and ED average myofiber stress decreases with decreasing injection  
179 volume (**Figure 4a**). In addition, the standard deviation of the myofiber stress also decreased  
180 substantially with decreasing injection volume and approaches the values in NO-RESIDUAL.  
181 Correspondingly, the myofiber stress field became more homogeneous near the injection sites  
182 (**Figure 4b**).

183

## 184 **2.6 Effect on ventricular volume**

185 The injections had little effects on both EDV and ESV in RESIDUAL and NO-RESIDUAL.  
186 Only in RESIDUAL was the EDV slightly smaller (198 ml) than BASELINE (201ml).

187

## 188 **3. DISCUSSIONS**

### 189 **3.1 Myofiber stretch and stress heterogeneity**

190 Although the global averaged myofiber stress became elevated when residual stress due to the  
191 injection was present, this increase was associated with a greater increase in its standard  
192 deviation. As such, the principal finding of our simulation is the increase in heterogeneity of the  
193 myofiber stretch and stress fields when residual stress is present, but not in the overall increase in  
194 myofiber stress. Specifically, the presence of residual stress produced a regular pattern of low  
195 myofiber stretch between injections in the LV mid wall, and high myofiber stretch extending



196 from the injections towards the endocardium and epicardium (**Figures 2** and **3**). The less than  
197 unity myofiber stretch between the injections at ED and ES implies that the midwall myofibers  
198 were compressed or “unloaded” throughout the cardiac cycle. This result can be explained by  
199 considering the myofiber orientation across the LV wall (**Figure 1b**). Because myofibers are  
200 oriented circumferentially at the midwall, they were compressed by the expanding voids that  
201 accommodated the injections. Contrastingly, the expanding voids also stretch the obliquely-  
202 oriented sub-endocardial and sub-epicardial myofibers.

203 The transmurally elongated ellipsoidal shape of the injection in the unloaded configuration  
204 (**Figure 1b**) is a consequence of (a) our assumption of a spherical void and (b) the anisotropic  
205 material behavior of the myocardium. Given that the LV wall is stiffest in the myofiber direction  
206 in our material model (Guccione et al., 1991), and the myofiber runs circumferentially at the LV  
207 mid wall, the compressive force acting on the initially spherical injections is therefore greatest  
208 along the circumferential direction of the LV wall. As a result, the injections were compressed in  
209 the circumferential direction of the LV wall. To preserve the injection volumes (as hydrogel is  
210 incompressible), the injections became elongated in the transmural direction.

211 Given that the contractive force generated by the myocytes is directly related to the sarcomere  
212 length (Guccione et al., 1993; ter Keurs et al., 1980), the decrease in mid-wall sarcomere length  
213 (reflected by a decrease in myofiber stretch) should, in principle, decrease the contractive force  
214 generated in that region. This effect is apparent in **Figure 3**, which shows a reduced mid-wall  
215 ES myofiber stress in RESIDUAL.

216 Another important effect of the injection-induced residual stress is evidenced by the fact that  
217 myofiber stretch is much less affected than myofiber stress at ED. This result is possible only if  
218 stress components transverse to the fiber direction are changed to balance the change in myofiber  
219 stress. Consequently, the myocardium supports a very different state of stress: one with  
220 potentially high shear components, and tension in direction normal to the fiber direction (Table  
221 1). If cross-fiber sensor located at the Z-disk is indeed present, as suggested by Russell et al.  
222 (2010), this difference (in stress state) may also potentially play a critical role in affecting tissue  
223 growth.

224 Last, it must be pointed out that the total prescribed injection volume of 0.24 ml is relatively  
225 small when compared to other computational models of injection treatment which have larger  
226 injection volumes e.g. ~ 5ml (Wall et al., 2006; Wenk et al., 2009) and ~ 9.4ml (Kortsmit et al.,  
227 2012). We did not increase the injection volume because doing so would lead to a highly  
228 distorted mesh near the injections, which would cause numerical instability. As a result, without  
229 the presence of residual stresses (NO-RESIDUAL), the injections have little effects on the global  
230 averaged myofiber stress and stretch as seen in Table 1.

231

### 232 **3.3 Ventricular volume change**

233 The little effect on EDV and ESV in RESIDUAL and NON-RESIDUAL is due to the small  
234 amount of injection prescribed in our models as discussed above. In other computational models  
235 of injection treatment (Wall et al., 2006; Wenk et al., 2009), a larger injection volume produced  
236 a greater effect on EDV and ESV.

237

### 238 **3.4 Limitations**

239 The key limitation of this model is the assumption of spherical voids that have a radius of 1mm  
240 in the myocardium, which of course, is an idealization. The void is most likely not perfectly  
241 spherical and uniform in size. Moreover, the inflation of voids during the injection process could  
242 be further complicated by any fracture planes the hydrogel could force open during injection. If  
243 all these complications are present, the resultant shape of the injection would most likely be  
244 different from our model prediction. For example, the injection of Methacrylated Hyaluronic  
245 Acid in normal ovine heart was found to be elongated circumferentially in the myofiber direction  
246 (Kichula et al., 2013) as opposed to our model's prediction that the injection is elongated in the  
247 transmural direction. Since residual stress can only be present if there is a misfit between the  
248 injection and the void, the degree of residual stress is sensitive to the void-to-injection size ratio  
249 (**Figure 4**) and how the void deforms and expands with injection. Experimental studies providing  
250 information on the shape and sizes of the myocardial voids could be performed in the future so  
251 that the degree and effects of residual stress can be better quantified.

252

253 **3.5 Summary**

254 In conclusion, we have described the first model that incorporates the effects of residual stress  
255 introduced by the injection of materials into the LV. Our results show that the stress and stretch  
256 fields near the injection region became more heterogeneous, whereby myofibers between the  
257 injections were unloaded and myofibers between the injections and both endocardium and  
258 epicardium were pre-stretched. These results are preliminary and models that incorporate more  
259 detailed microstructural information are needed to shed light on the possible role of residual  
260 stress in the reported therapeutic effects associated with the injection treatment.

261

262 **4. ACKNOWLEDGEMENT**

263 This study was supported by National Heart, Lung, and Blood Institute Grants R01-HL-077921,  
264 R01-HL-118627 (to J. M. Guccione), and by a Marie-Curie International Outgoing Fellowship  
265 within the 7th European Community Framework Programme (M. Genet). We would like to  
266 thank Pamela Derish in Department of Surgery at UCSF for proofing the manuscript

267 **5. REFERENCES**

- 268 Christman, K.L., Fok, H.H., Sievers, R.E., Fang, Q., Lee, R.J., 2004. Fibrin glue alone and  
 269 skeletal myoblasts in a fibrin scaffold preserve cardiac function after myocardial infarction.  
 270 *Tissue Eng.* 10, 403–9.
- 271 Frank, J.S., Langer, G. a, 1974. The myocardial interstitium: its structure and its role in ionic  
 272 exchange. *J. Cell Biol.* 60, 586–601.
- 273 Guccione, J.M., McCulloch, A.D., Waldman, L.K., 1991. Passive material properties of intact  
 274 ventricular myocardium determined from a cylindrical model. *J. Biomech. Eng.* 113, 42–55.
- 275 Guccione, J.M., Waldman, L.K., McCulloch, A.D., 1993. Mechanics of active contraction in  
 276 cardiac muscle: part II-cylindrical models of the systolic left ventricle. *J. Biomech. Eng.*  
 277 115, 82–90.
- 278 Jiang, X.J., Wang, T., Li, X.Y., Wu, D.Q., Zheng, Z. Bin, Zhang, J.F., Chen, J.L., Peng, B.,  
 279 Jiang, H., Huang, C., Zhang, X.Z., 2009. Injection of a novel synthetic hydrogel preserves  
 280 left ventricle function after myocardial infarction. *J. Biomed. Mater. Res. A* 90, 472–7.
- 281 Kichula, E.T., Wang, H., Dorsey, S.M., Szczesny, S.E., Elliott, D.M., Burdick, J. a, Wenk, J.F.,  
 282 2013. Experimental and Computational Investigation of Altered Mechanical Properties in  
 283 Myocardium after Hydrogel Injection. *Ann. Biomed. Eng.*
- 284 Kortsmit, J., Davies, N.H., Miller, R., Macadangdang, J.R., Zilla, P., Franz, T., 2012. The effect  
 285 of hydrogel injection on cardiac function and myocardial mechanics in a computational  
 286 post-infarction model. *Comput. Methods Biomech. Biomed. Engin.*
- 287 Landa, N., Miller, L., Feinberg, M.S., Holbova, R., Shachar, M., Freeman, I., Cohen, S., Leor, J.,  
 288 2008. Effect of injectable alginate implant on cardiac remodeling and function after recent  
 289 and old infarcts in rat. *Circulation* 117, 1388–96.
- 290 Lee, L.C., Wall, S.T., Klepach, D., Ge, L., Zhang, Z., Lee, R.J., Hinson, A., Gorman, J.H.,  
 291 Gorman, R.C., Guccione, J.M., 2013a. Algisyl-LVR™ with coronary artery bypass grafting  
 292 reduces left ventricular wall stress and improves function in the failing human heart. *Int. J.*  
 293 *Cardiol.* 168, 2022–2028.
- 294 Lee, L.C., Zhihong, Z., Hinson, A., Guccione, J.M., 2013b. Reduction in left ventricular wall  
 295 stress and improvement in function in failing hearts using Algisyl-LVR. *J. Vis. Exp.* 1–6.
- 296 Nelson, D.M., Ma, Z., Fujimoto, K.L., Hashizume, R., Wagner, W.R., 2011. Intra-myocardial  
 297 biomaterial injection therapy in the treatment of heart failure: Materials, outcomes and  
 298 challenges. *Acta Biomater.* 7, 1–15.

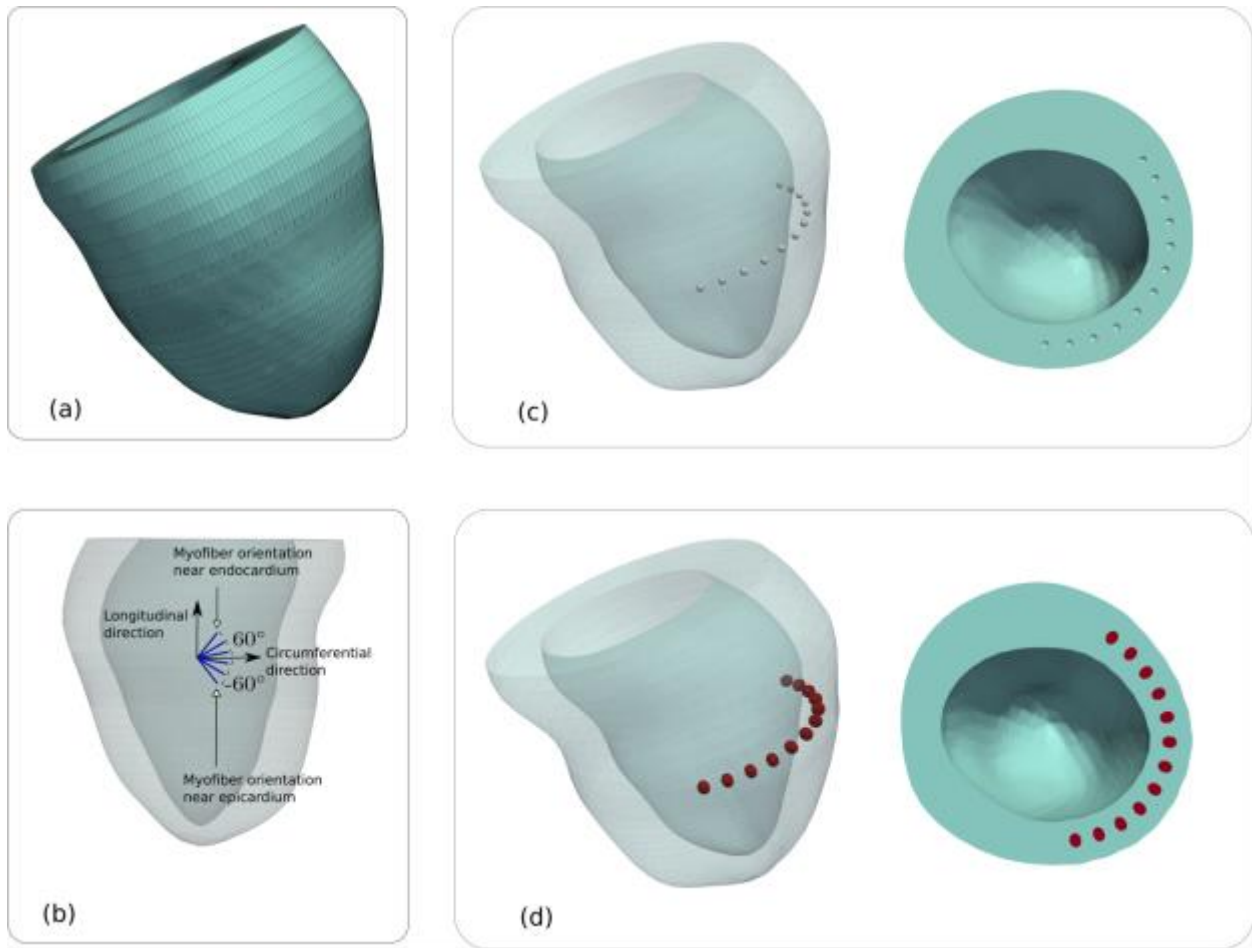
- 299 Russell, B., Curtis, M.W., Koshman, Y.E., Samarel, A.M., 2010. Mechanical stress-induced  
300 sarcomere assembly for cardiac muscle growth in length and width. *J. Mol. Cell. Cardiol.*  
301 48, 817–23.
- 302 Streeter, D.D., Spotnitz, H.M., Patel, D.P., Ross, J., Sonnenblick, E.H., 1969. Fiber orientation in  
303 the canine left ventricle during diastole and systole. *Circ. Res.* 24, 339–47.
- 304 Sun, K., Stander, N., Jhun, C.S., Zhang, Z., Suzuki, T., Wang, G.Y., Saeed, M., Wallace, A.W.,  
305 Tseng, E.E., Baker, A.J., Saloner, D., Einstein, D.R., Ratcliffe, M.B., Guccione, J.M., 2009.  
306 A computationally efficient formal optimization of regional myocardial contractility in a  
307 sheep with left ventricular aneurysm. *J. Biomech. Eng.* 131, 111001.
- 308 Ter Keurs, H.E., Rijnsburger, W.H., van Heuningen, R., Nagelsmit, M.J., 1980. Tension  
309 development and sarcomere length in rat cardiac trabeculae. Evidence of length-dependent  
310 activation. *Circ. Res.* 46, 703–714.
- 311 Wall, S.T., Walker, J.C., Healy, K.E., Ratcliffe, M.B., Guccione, J.M., 2006. Theoretical impact  
312 of the injection of material into the myocardium: a finite element model simulation.  
313 *Circulation* 114, 2627–35.
- 314 Wenk, J.F., Klepach, D., Lee, L.C., Zhang, Z., Ge, L., Tseng, E.E., Martin, A., Kozerke, S.,  
315 Gorman, J.H., Gorman, R.C., Guccione, J.M., 2012. First evidence of depressed  
316 contractility in the border zone of a human myocardial infarction. *Ann. Thorac. Surg.* 93,  
317 1188–93.
- 318 Wenk, J.F., Wall, S.T., Peterson, R.C., Helgerson, S.L., Sabbah, H.N., Burger, M., Stander, N.,  
319 Ratcliffe, M.B., Guccione, J.M., 2009. A method for automatically optimizing medical  
320 devices for treating heart failure: designing polymeric injection patterns. *J. Biomech. Eng.*  
321 131, 121011.
- 322
- 323
- 324
- 325
- 326
- 327

328 **6. TABLES**

329 **Table 1:** Myofiber and cross-myofiber stretch and stress (average  $\pm$  standard deviation at end-  
 330 diastole (ED) and end-systole (ES). Refer to text description of BASELINE, RESIDUAL and  
 331 NO-RESIDUAL.

|  |    | <b>BASELINE</b> | <b>RESIDUAL</b> | <b>NO-RESIDUAL</b> |
|--|----|-----------------|-----------------|--------------------|
| <b>Myofiber stretch</b>                | ED | 1.12 $\pm$ 0.02 | 1.11 $\pm$ 0.04 | 1.12 $\pm$ 0.02    |
|  | ES | 0.97 $\pm$ 0.03 | 0.97 $\pm$ 0.04 | 0.97 $\pm$ 0.03    |
| <b>Cross Myofiber stretch</b>          | ED | 1.12 $\pm$ 0.05 | 1.11 $\pm$ 0.06 | 1.12 $\pm$ 0.04    |
|  | ES | 1.00 $\pm$ 0.06 | 1.01 $\pm$ 0.07 | 1.01 $\pm$ 0.07    |
| <b>Myofiber stress<br/>(kPa)</b>       | ED | 6.9 $\pm$ 4.6   | 11.2 $\pm$ 48.8 | 6.7 $\pm$ 4.6      |
|  | ES | 30 $\pm$ 15     | 35.1 $\pm$ 50.9 | 30 $\pm$ 15        |
| <b>Cross Myofiber stress<br/>(kPa)</b> | ED | 3.9 $\pm$ 3.8   | 8.1 $\pm$ 50.1  | 3.8 $\pm$ 3.8      |
|  | ES | 8.1 $\pm$ 8.2   | 13.4 $\pm$ 57.9 | 8.1 $\pm$ 8.3      |

332 7. FIGURES



333

334 **Figure 1**(a): Finite element mesh of the patient-specific LV. (b): Transmural variation of the myofiber orientation.  
 335 Left ventricular mesh with (c): 12 spherical voids each having a 1mm radius and (d): injections (red) filling up the  
 336 void spaces. Notice that the injections are no longer spherical and are slightly elongated transmurally.

337

338

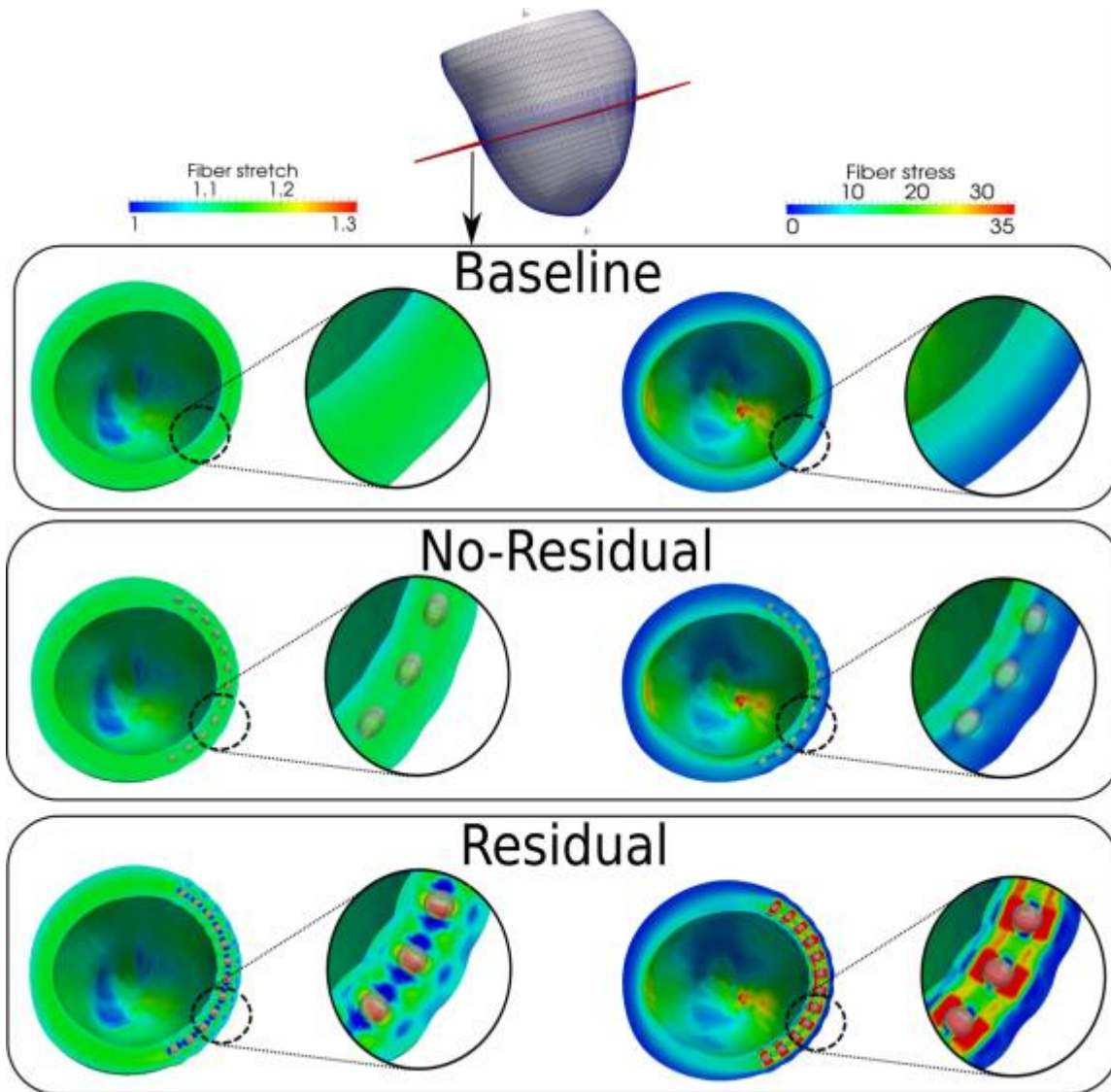
339

340

341

342

343



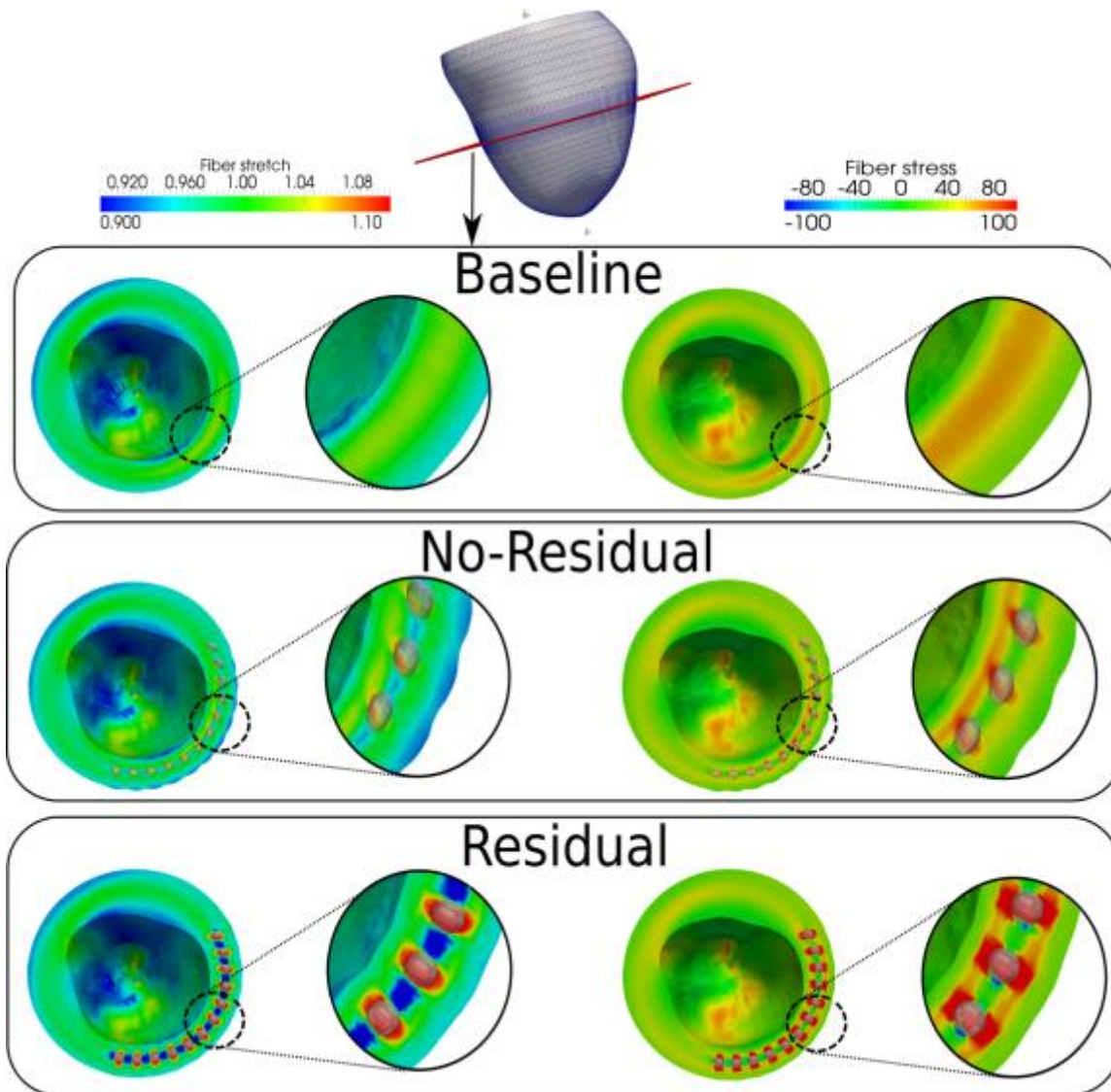
344

345 **Figure 2:** Comparison of fiber stretch and stress for the baseline, no-residual and residual cases at end-of-diastole.

346 Cutting plane is shown in red at the top picture. Unit of fiber stress is kPa.

347





348

349 **Figure 3:** Comparison of fiber stretch and stress for the baseline, no-residual and residual cases at end-of-systole  
 350 Cutting plane is shown in red at the top picture. Arrow in the residual case indicates the reduced midwall end-  
 351 systolic myofiber stress. Unit of fiber stress is kPa.

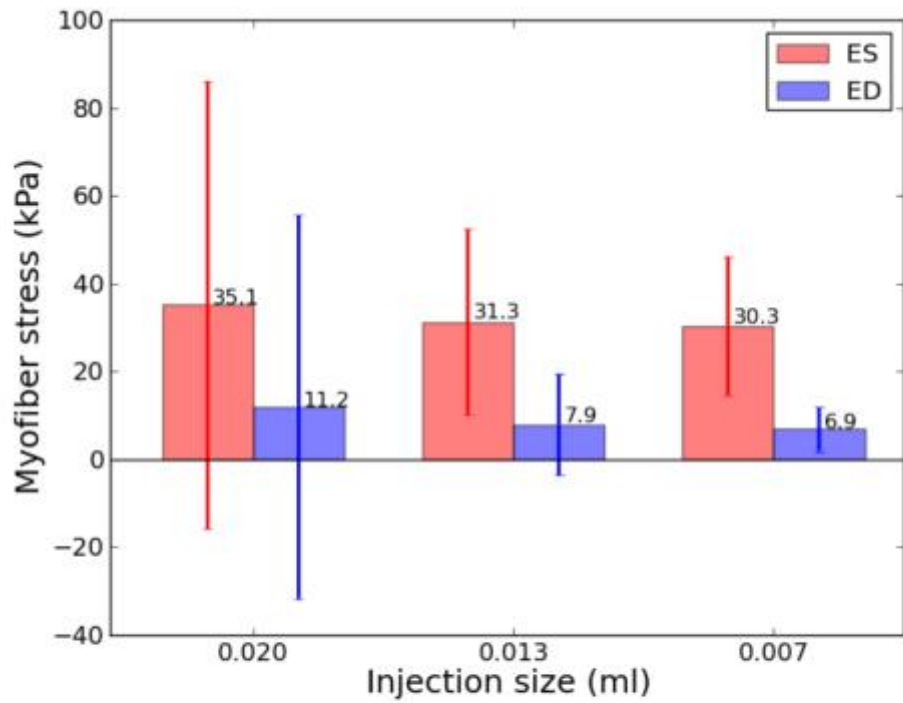
352

353

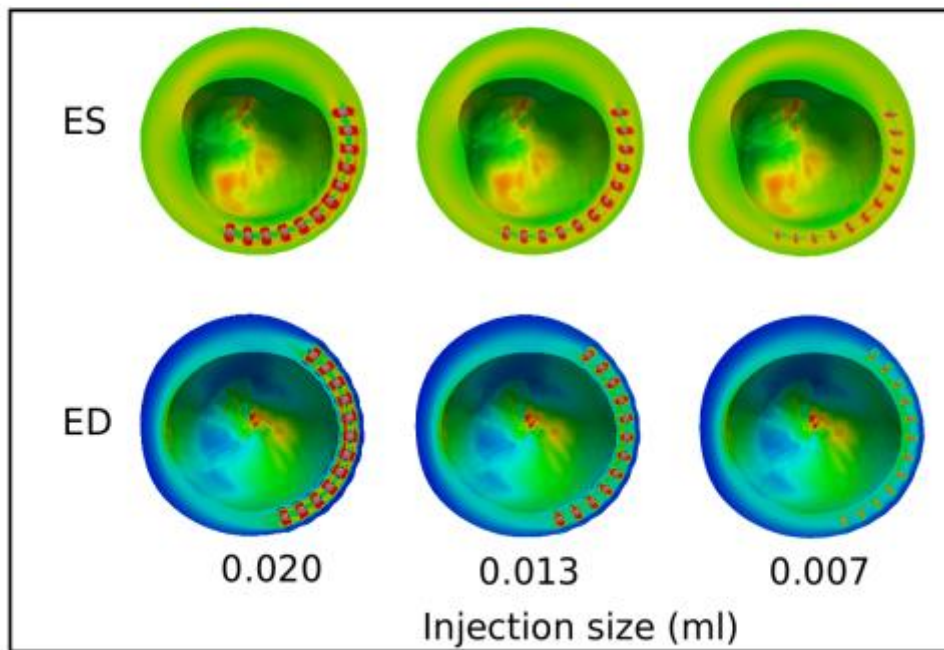
354

355

356



(a)



(b)

357

358 **Figure 4:** Effects of injection size (with constant void size) on (a) global myofiber stress and (b) regional myofiber  
 359 stress near the injection sites. Mean values of myofiber stress are given on top of each bar in (a). Refer to Fig. 2 and  
 360 3's legend for ED and ES regional myofiber stress in (b), respectively.